Published in final edited form as:
Int J Cancer. 2012 October 1; 131(7): E1088–E1099. doi:10.1002/ijc.27615.

Progastrin overexpression imparts tumorigenic/metastatic potential to embryonic epithelial cells: phenotypic differences between transformed and non-transformed stem cells

Shubhashish Sarkar[1,*], **Carla Kantara**[1,4,*], **Ixiu Ortiz**[1], **Rafal Swiercz**[1,4], **Joyce Kuo**[1], **Robert Davey**[2], **Kenneth Escobar**[3], **Robert Ullrich**[4], and **Pomila Singh**[1,4]

[1]Department of Neuroscience and Cell Biology, UtmbHealth, Galveston, TX

[2]Department of Microbiology, UtmbHealth, Galveston, TX

[3]Department of Pathology, UtmbHealth, Galveston, TX

[4]Sealy Cancer Center, UtmbHealth, Galveston, TX

Abstract

We recently reported that overexpression of progastrin in embryonic epithelial cells (HEKmGAS-cells) increased proliferation of the cells, compared to that of control HEKC-cells. Here we report the novel finding that tumorigenic and metastatic potential of HEKmGAS cells is also increased significantly, compared to that of HEKC cells. Cell-surface associated annexinA2 (CS-ANXA2) binds progastrin and is over-expressed on cancer-cells, allowing us to successfully use fluorescently-labeled progastrin-peptide for enumerating metastatic lesions of transformed/cancer cells *in vivo*. Next, we examined the hypothesis that increased tumorigenic/metastatic potential of isogenic HEKmGAS vs HEKC cells maybe due to transformed-phenotype of stem-cells. FACSorting/FACScanning of cells demonstrated significant increases in percent DCLK1/Lgr5 positive stem-cells, co-expressing CD44/CS-ANXA2, in HEKmGAS vs HEKC-cells. Distinct differences were noted in morphology of HEKC vs HEKmGAS spheroidal growths on non-adherent cultures (selective for stem cells). HEKC-spheroids were rounded with distinct perimeters (basement membranes?), while HEKmGAS-spheroids were amorphous, with no perimeters. Relative levels of DCLK1/Lgr5/CD44 and AnnexinA2/β-catenin/*p*NFκBp65/metalloproteinases were significantly increased in HEKmGAS vs HEKC-cells, growing either as mono-layer cultures, 3D-spheroids (*in vitro*), or xenografts (*in vivo*). Interestingly, HEKC-cells enriched for CS-ANXA2, developed amorphous spheroids, while down-regulation of ANXA2 in HEKmGAS-clones, resulted in loss of matrixmetalloproteinases and re-formation of rounded spheroids, suggesting high levels of CS-ANXA2/matrixmetalloproteinases may impact spheroid morphology. Down-regulation of DCLK1 significantly attenuated activation of β-catenin, with loss of proliferation of HEKmGAS and HEKC-cells, suggesting DCLK1 is required for maintaining proliferation of cells.

Conclusions—Our results suggest the novel possibility that transformed stem-cells, unlike non-transformed stem-cells, co-express stem-cell-markers DCLK1 and CD44 with CS-ANXA2.

Correspondence: Pomila Singh, Professor, Department of Neuroscience and Cell Biology, University of Texas Medical Branch, 10.104 Medical Research Bldg, 301 University Blvd, Route 1043, Galveston, TX 77555-1043, posingh@utmb.edu, Office: 409-772-4842, FAX: 409-772-3222.
*shared first authorship

Disclosures: No conflict of interest to report.

Keywords

DCLK1; CD44; β-catenin; Stem-Cells; annexinA2

INTRODUCTION

Exogenous/autocrine gastrins up-regulate proliferation/co-carcinogenesis of gastrointestinal and pancreatic cancers (1). Normally, only processed and amidated forms of gastrins (G17/G34) are present in circulation; however in specific disease states, elevated levels of progastrins are detected (1). Progastrin (PG) and glycine-extended-gastrins are expressed by colonic/ovarian/pancreatic/lung cancers (1). Importantly, down-regulation of gastrin gene (and hence PG) results in loss of clonogenecity/tumorigenicity of cancer cells (2,3). We and others have confirmed potent proliferative/anti-apoptotic effects of PG peptides on target cells *in vitro* and *in vivo* (4–7). Transgenic mice over-expressing PG develop colonic adenomas/adenocarcinomas in response to azoxymethane (8–10). Thus both endocrine/autocrine PG contribute to tumorigenic potential of epithelial cells.

Our results strongly suggest that AnnexinA2 (ANXA2) represents a non-conventional 'receptor' for PG/gastrin peptides (7,11,12), and mediates activation of p65NFκB/β-catenin in response to PG (12). ANXA2 expression is required for inducing proliferative/anti-apoptotic effects of PG on target cells *in vitro* (7,11,12) and *in vivo* (12). We additionally discovered that cell-surface-ANXA2 (CS-ANXA2) mediates endocytotic internalization of PG, which is required for measuring biological effects of PG (12,13).

We recently reported that over-expression of gastrin-cDNA (PG) in HEK293-cells (HEKmGAS-cells) significantly increased activation/expression of NFκBp65/β-catenin, associated with increased proliferation of the cells (12). In the current studies we examined if the dramatic changes measured in HEKmGAS-cells, in response to autocrine PG, can perhaps increase clonogenic/tumorigenic potential of cells. Our results demonstrate for the first time that over-expression of autocrine-PG in embryonic HEK293-cells, imparts tumorigenic/metastatic potential to cells.

We previously reported a significant increase in the relative expression levels of DCAMKL+1/CD44/ANXA2 in HEKmGAS vs HEKC-cells (12); in the current studies we examined if % cells expressing the indicated markers are also elevated. For the purpose of our studies however, we have used the term DCLK1, instead of DCAMKL+1, which represents the new up-dated nomenclature for this protein. A critical role of CS-ANXA2 in metastasis of epithelial-cancers has been reported (14–16). Since HEKmGAS-cells developed metastatic potential, we examined the possibility if HEKmGAS derived stem-cells had acquired the ability to co-express CS-ANXA2. We report for the first time that a high % of CS-ANXA2 positive HEKmGAS-cells, co-expressed stem-cell-markers, CD44 and DCLK1, which may represent the transformed phenotype of stem-cells.

Non-adherent cell cultures, select for growth of stem-cells as spheroids (17). Surprisingly, we discovered that HEKC-cells formed well-rounded spheroids with a distinct, rim-like, perimeter encircling the spheroid, while HEKmGAS-cells formed amorphous spheroids, without a distinct rim-like perimeter. Elevated levels of CS-ANXA2 are associated with increased expression of matrixmetalloproteinases (MMPs) and invasion (18). Since we measured high levels of CS-ANXA2/MMPs in HEKmGAS vs HEKC-cells (current studies), we examined the impact of altering expression levels of CS-ANXA2/ANXA2 on spheroid-morphology. Our results demonstrate that either down-regulation of ANXA2/CS-ANXA2, or enrichment of cells for CS-ANXA2, significantly altered spheroid-morphology,

suggesting the novel possibility that phenotypic differences in spheroidal growths may predict tumorigenic/metastatic potential of cells.

MATERIAL AND METHODS

Details of materials and methods are provided in Supplementary Methods (Supplementary-Methods) (A-L).

Specific reagents used are described in Supplementary-Methods (A).

Cell-culture and generation of PG-expressing HEKmGAS-clones

HEK293 and HCT-116 cells, obtained from ATCC, were maintained in DMEM/F12 as described (11,12). Eukaryotic expression plasmid containing full-length coding sequence for triple-double mutant hGAS gene (R57A-R58A, K74A-K75A, R94A-R95A) (9), was transfected into HEK293-cells to create stably-expressing hPG-clones (HEKmGAS), and confirmed, as described (12). Vector-transfected clones (HEKC) were used as control.

In vitro growth assays and *in vivo* tumorigenic/metastatic assays

Cell growth was measured in an MTT (3–4,5-Dimethylthiazol-2-yl) or soft-agar assay (clonogenic growth) as described (2). Cells were inoculated in athymic (SCID/Nude) mice to grow either sub-dermal xenografts, or orthotopic-growths in cecum, or metastatic-growths in liver/lung after intrasplenic-inoculations, as detailed in Supplementary-Methods (B). Majority of mice inoculated with HEKC-clones did not show palpable growths even after 6wks. After 4–6wks from time of inoculation, tumors were harvested, dissected free of host tissue, patted dry and weighed. Where indicated, mice were also inoculated with cells, stably expressing firefly-luciferase (Luc); Luc-expressing tumors were imaged *in vivo*, as described in Supplementary-Methods (C,D). HEKmGAS, HEKC and HCT-116 cells express CS-ANXA2 and bind PG with high-affinity (11,12), followed by internalized (12,13). Based on a previous report (19), we confirmed binding/biological effects of PG26 (26 amino-acids at C-terminal end of PG). PG26-peptide was conjugated to Lys-(5/6-FAM) at N-terminal end (FAM-PG26) by Peptide Core Facility (http://www.tucf.org). The high relative-binding-affinity of FAM-PG26 for displacing binding of ^{125}I-rhPG to HEKC-cells was confirmed as previously described (6). Internalization of FAM-PG26 was also confirmed in target-cells, as a functional readout (Supplementary-Fig 1A–C). FAM-PG26 was then used for detecting primary/metastatic tumors as described in Supplementary-Methods (E).

Co-immunoprecipitation of ANXA2 with anti-PG-Antibodies (Abs) in tissue samples is described in Supplementary-Methods (F).

Analysis of % cells positive for stem-cell-markers (DCLK1, Lgr5, CD44) and/or ANXA2/CS-ANXA2. Three methods (Methods I–III) were used as detailed in Supplementary-Methods (G).

In Vitro growth of cells as 3D-spheroids, and processing of the spheres for staining are detailed in Supplementary-Methods (H).

Western Blot (WB) analysis of cells growing either as 2D-cultures, 3D-spheroids or sub-dermal tumors in mice, was performed as described in Supplementary-Methods (I).

Transient-transfection of cells with oligonucleotides is described in Supplementary-Methods (J).

Transient-transfection of cells with ANXA2-shRNA plasmids for down-regulation of endogenous ANXA2 is described in Supplementary-Methods (K).

Statistical analysis of data is described in Supplementary-Methods (L).

RESULTS

Clonogenic/tumorigenic potential of HEKmGAS vs HEKC clones

HEKmGAS-clones were confirmed to stably express full-length PG as previously described (12). Clonogenic growth of HEKmGAS/HEKC-clones on soft-agar is presented in Fig 1Ai. Number of colonies formed/dish from HEKmGAS-clones (mGAS1-3) vs an HEKC-clone increased from ~2-fold (1% FCS) to >4-fold (10% FCS) (Fig 1Aii). Tumorigenic-potential of cells was examined *in vivo* as described in Methods. Representative sub-dermal tumors from nude mice are shown in Fig 1Bi. Only 20% mice inoculated with HEKC-cells developed palpable tumors (Fig 1Bii), suggesting negligible tumorigenic potential of HEKC-cells, similar to wtHEK293-cells. All mice inoculated with HEKmGAS/HCT-116 cells formed sub-dermal tumors with almost identical weights (Figs 1Bii–iii). Thus overexpression of PG in the background of HEK293-cells resulted in significantly increasing tumorigenic potential of cells. HEKmGAS-Luc cells, stably expressing firefly-luciferase, were inoculated orthotopically (ORT) within the cecal wall and imaged as described in Methods (Fig 1Ci). Orthotopic-tumors were slightly smaller than sub-dermal tumors (P), but gave rise to metastatic (MET) growths in the liver (Figs 1Ci–ii). These results suggest that orthotopic tumors can potentially metastasize, mimicking metastatic spread of *in situ* colorectal-adenocarcinomas (CRC). Intrasplenic inoculation of HEKmGAS/HEKmGAS-Luc cells resulted in metastatic lesions in the livers, within 3–4wks of inoculation; representative visual (Fig 1Di) and bioluminescent (Fig 1Dii) images of HEKmGAS/HEKmGAS-Luc tumors, are shown, respectively. Presence of metastatic-lesions in liver/lung was confirmed by H&E and IF staining (Supplementary-Figs 2A–C). Since HEKmGAS-cells express autocrine-PG, both primary (Supplementary-Fig 2Di) and metastatic-lesions (Supplementary-Figs 2B–E) were positive for PG staining, while sub-dermal HEKC-tumors were negative (Supplementary-Fig 2Di); normal (NOR) livers from mice were negative for PG expression, as expected (Supplementary-Fig 2E). Co-immunoprecipitation of ANXA2 with PG was confirmed in Western-Blots of sub-dermal HEKmGAS-tumors (Supplementary-Fig 2Dii). ANXA2 strongly co-localized with PG in HEKmGAS metastatic-lesions, confirming metastasis to lungs/liver (Supplementary-Figs 2B,C).

Primary/metastatic lesions diagnosed with fluorescently-labeled PG

High-affinity-ligands of CS-ANXA2 have been developed to detect tumors (20). Since PG binds CS-ANXA2 with high-affinity (7,11,12), we examined if labeled-PG peptides can detect primary/metastatic-tumors. FAM-PG26, confirmed to be biologically active (Supplementary-Fig 1), was used for reasons described in Methods. FAM-PG26, injected intra-tumorally, was retained for ~30min (representative image at 15min shown in Fig 2Ai). Tail-vein injection of FAM-PG26 resulted in increasing accumulation of peptide at the tumor-site from 0–15min followed by a rapid decline; representative images from a single mouse at 0,5,15,30 min, after tail-vein injection of FAM-PG26, are shown in Fig 2Bi; relative fluorescence-intensity from 3 mice are presented in Fig 2Bii. HCT116-xenografts also accumulated FAM-PG26 peptide from 0–15min, followed by a rapid decline; representative image at 15min is shown in Fig 2Aii. Representative images from resected tumors after 15min of tail-vein injection with either FITC (used as control) or FAM-PG26 are shown in Figs 2Ci–ii, demonstrating focal uptake/retention of labeled-peptide. Metastatic lesions in liver and lung specimens were detected after 15min of FAM-PG26

injection (Figs 2Di–ii); once again the lesions were positive for FAM-PG26 up-take in focal areas.

Up-regulation of % cells expressing CS-ANXA2/ANXA2 and stem-cell-markers in HEKmGAS vs HEKC-cells

Three separate methods (Methods I-III) (described in Supplementary-Fig 3A) were used to define % cells positive for stem-cell-markers and CS-ANXA2/ANXA2. Representative staining of cells growing on cover slips, for the indicated markers (Method-II) are presented in Fig 3A. Representative results with FACSorting of cells (Method-III), using antibodies against stem-cell-markers (DCLK1/CD44/Lgr5), and ANXA2, are presented in Supplementary-Fig 3B. Results with the three separate methods (labeled as I, II, and III) from 2–3 separate experiments, are presented as % cells positive for the indicated proteins in Fig 3B. Percent cells positive for ANXA2/CS-ANXA2 and the indicated stem-cell-marker(s) were significantly increased in HEKmGAS vs HEKC-cells (Fig 3B; Supplementary-Fig 3B). Importantly, results of the three methods (I, II, and III) gave similar results.

High % of ANXA2 positive cells co-expresses DCLK1/CD44

IF staining of cells, by Method-II, suggested that significant % of HEKC/HEKmGAS-cells co-express ANXA2 with a stem-cell-marker (Fig 4A). To further confirm this finding, cells were FACSorted with Anti-ANXA2-Abs, and cells positive (ANXA2+) or negative (ANXA2-) for CS-ANXA2, were stained for stem-cell-markers (Fig 4B). HEKC-cells were negative, while HEKmGAS-cells were positive for PG staining, irrespective of ANXA2 status; PG strongly co-localized with ANXA2 in HEKmGAS-ANXA2(+) cells (Fig 4B; Supplementary-Fig 4A). ANXA2(-) cells stained poorly while ANXA2(+) cells stained strongly for ANXA2 (Fig 4B). Staining intensity for Lgr5/DCLK1/CD44 was highest in ANXA2(+) HEKmGAS cells (Fig 4B; Supplementary-Figs 4B,C). Percent cells co-expressing ANXA2 and a stem-cell-marker, were quantified by FACScanning (as described in Methods), and results are presented in Figs 4C–E. Significantly higher % of HEKmGAS-cells co-expressed ANXA2 and the indicated stem-cell-marker (Fig 4C). Results were recalculated as % ANXA2(+) cells which co-expressed DCLK1/CD44/Lgr5; surprisingly almost all ANXA2(+) cells co-expressed CD44 in both HEKC/HEKmGAS cells, while a lower % co-expressed DCLK1/Lgr5 (Fig 4D). Percent cells positive for a stem-cell-marker along with CS-ANXA2 were also analyzed by FACScan (Fig 4E). Once again almost all CD44(+) cells co-expressed CS-ANXA2, while ~50–80% of DCLK1(+) cells co-expressed CS-ANXA2; much lower % of Lgr5(+) cells co-expressed CS-ANXA2 (Fig 4E). Importantly, significantly higher % of DCLK1/Lgr5 positive HEKmGAS-cells co-expressed CS-ANXA2 (Fig 4E), suggesting that combined expression of these proteins may impact tumorigenic/metastatic potential of cells.

Morphological differences in spheroidal growths of HEKC/HEKmGAS cells

Stem-cells from normal/cancerous tissues have inherent potential of amplifying and forming spheroidal structures in non-adherent cultures (17,21). Since stem-cell-populations were significantly up-regulated in HEKmGAS-cells, we examined possible increase in rate of spheroid-formation by HEKmGAS vs HEKC-cells. Both HEKC/HEKmGAS cells formed spheroidal structures at days 5–6, with significant morphological differences (Fig 5Ai). Non-adherent growth of HEKmGAS-cells was more pronounced at initial time-points (24–48h), but appeared to even out by day 6 (Fig 5Ai). HEKC-spheroids appeared well-rounded with a distinct, rim-like, perimeter (arrows), while HEKmGAS-spheroids lacked a distinct, rim-like, perimeter and were more amorphous in shape (Fig 5Ai). Total numbers of spheroidal structures were significantly higher in HEKmGAS vs HEKC-cells at all time-points. Data from two separate experiments at 24h and at day 6 are presented in Fig 5Aii. The size of the

HEKmGAS vs HEKC spheroids at different time-points, however, was not significantly different, as can be gauged from representative data presented in Fig 5Ai. Since wtHEKmGAS-spheroids were amorphous and appeared to be less well aggregated, especially at the periphery of the spheroids, we could not process intact HEKmGAS-spheroids for staining. Representative sections of HEKC-spheroids, stained with H&E (Fig 5Bi), and with specific-Abs (Fig 5Bii), are shown. Surprisingly, DCLK1(+) and Lgr5(+) cells were present along the periphery of the spheroids, while CD44(+) cells were present throughout the spheroids. None of the stem cells (positive for CD44/DCLK1), co-expressed ANXA2 in HEKC-spheroids, while clumps of HEKmGAS-spheroids, leftover after processing, co-expressed ANXA2 with CD44/DCLK1 (representative data shown in Supplementary-Fig 5A). Anti-Ki67-Abs stained HEKC-spheroidal cells both at the periphery and within the spheroids (Fig 5Bii), suggesting proliferating cells are present at the periphery and within the spheroids. DCLK1(+) cells were also observed mainly around the edges of sub-dermal tumors from HEKmGAS-cells (Supplementary-Fig 5B), suggesting that stem-cell-populations may be primarily present along the outer edges of tumors/spheroids (Fig 5B; Supplementary-Fig 5Bii). Focal areas of the sub-dermal tumors, derived from HEKmGAS-cells, were also heavily stained for CD44/ANXA2 by IHC, and the two proteins appeared to be expressed in the same areas (Supplementary-Fig 5C); IF staining highlighted significant co-expression of CD44 and ANXA2 in these focal areas at the outer edges of the sub-dermal tumors (Supplementary-Fig 5D).

Role of ANXA2 expression on spheroidal growths

We next examined the hypothesis that overexpression of CS-ANXA2/ANXA2 may have resulted in the inability of HEKmGAS-cells to form well-rounded spheroids. HEKC-cells expressing CS-ANXA2 were enriched by FACSorting with anti-ANXA2-Abs. Surprisingly, CS-ANXA2(+)HEKC-cells grew as amorphous-spheroids, while HEKC-cells negative for CS-ANXA2 continued to grow like wtHEKC-cells (Fig 5C). Alternatively, HEKmGAS-cells were down-regulated for ANXA2 expression by transiently transfecting the cells with ANXA2-shRNA plasmids. HEKmGAS-cells transfected with control-shRNA developed amorphous-spheroids, while HEKmGAS-cells down-regulated for ANXA2 formed more compact spheroids, which could be processed for sectioning/staining more successfully (Fig 5D). Importantly, MMP2/7 expression in HEKmGAS-spheroids, down-regulated for ANXA2 expression, was significantly attenuated compared to that in HEKmGAS-spheroids, treated with control-shRNA (Fig 5E), suggesting the possibility that ANXA2 may regulate secretion/expression of MMPs.

Relative expression of stem-cell-markers by HEKmGAS vs HEKC-cells

Based on our current and previous studies (12), we now know that PG over-expression in HEKmGAS-cells significantly up-regulates relative expression levels of stem-cell-markers and ANXA2 and activates β-catenin/NFκBp65. It is, however, not known if enhanced expression/activation is maintained in HEKmGAS-cells growing as spheroids/tumors. Cells growing either as 2D-cultures, 3D-spheroids or xenografts were processed for WB analysis. Representative data from 2–3 experiments are presented in Fig 6A; % change in the ratio of target proteins/β-actin in HEKC vs HEKmGAS-samples was determined, wherein the ratios obtained for HEKC-samples was arbitrarily assigned a 100% value (dashed lines in each panel of Fig 6B). Enhanced expression of DCLK1/Lgr5/CD44 and ANXA2/β-catenin/*p*NFκBp65 in HEKmGAS vs HEKC-cells was similarly increased in cells growing either as monolayer-cultures **(M)**, 3D-spheroids **(S)** or tumors **(T)** (Figs 6A,B). HEKmGAS-cells growing as spheroids/tumors expressed significantly higher levels of PG than cells growing as monolayer-cultures, suggesting the novel possibility that HEKmGAS-cells growing as 3D-structures (*in vitro/in vivo*) may increasingly express endogenous PG.

Down-regulation of DCLK1 attenuates activation of β-catenin and growth of HEKC/HEKmGAS cells in culture

Recent reports suggest that DCLK1 may play an important role in growth of cancer cells (22,23). Cells were treated with either DCLK1-siRNA or control-siRNA (Fig 6C). Even though HEKC-cells expressed low levels of DCLK1 (Figs 3B,6A), proliferation of both HEKC/HEKmGAS cells was significantly down-regulated in DCLK1-siRNA vs control-siRNA treated cells (Fig 6D), providing evidence that DCLK1 may play an important role in proliferation of immortalized/transformed HEK293-cells. These results for the first time suggest that DCLK1, may play a functional role in supporting proliferation of cells. Thus a possible cross-talk between stem-cell-markers and signaling pathways needs to be further examined in relation to proliferation/tumorigenesis of cells.

DISCUSSION

In the current studies, we demonstrate for the first time that PG expression in immortalized embryonic cells increases tumorigenic/metastatic potential of cells. Over-expression of autocrine PG, however, was not effective in transforming immortalized intestinal-epithelial cells (IEC-18) (24). It is thus possible that HEK293-cells, unlike IEC18-cells, are positive for an initiating event, and over-expression of PG facilitates transformation of HEK293-cells. Transgenic mice over-expressing PG are at an increased risk for colon-carcinogenesis in response to azoxymethane (8–10). Gastrin gene (PG) expression is normally repressed in colonic epithelial-cells, but is increasingly expressed during hyperplastic/adenoma/carcinoma sequence of colon-carcinogenesis (1). It is thus possible that increasing expression of autocrine PG contributes to colon-carcinogenesis of ‘initiated’ cells; our current findings provide evidence for this novel possibility.

Membrane associated CS-ANXA2, recently discovered as a novel receptor for PG (7,11,12), binds several ligands and is present on endothelial cells/keratinocytes/epithelial cancer cells (14–16,18,25,26). Functional significance of CS-ANXA2 in proliferation/metastasis of cancer-cells is becoming increasingly evident (14–16,18,25). Progression of pancreatic/breast cancer disease is associated with a switch from cytoplasmic to cell-surface expression of ANXA2 (27,28). Exosomes, secreted by cancer cells, contain ANXA2 (29), and may be the source of CS-ANXA2 and soluble-ANXA2 measured in conditioned-medium/serum of cancer-cells/patients (26,29–31). We also measured 2–3fold increase in percent cells positive for CS-ANXA2 in HEKmGAS vs HEKC-cells (Fig 3), supporting the notion that wounding/immortalization/oncogenic transformation is conducive to increasing CS-ANXA2 on epithelial cells (15,16,18,25–29,32,current studies).

Radiolabeled peptide-ligands for membrane-receptors are being developed for diagnostic/therapeutic purposes (33). We demonstrate for the first time that iv injected labeled-PG-peptide (FAM-PG26) effectively and specifically homed to primary/metastatic HEKmGAS/HCT-116 tumors within 5–15min of injection (Fig 2). Even though HEKmGAS/HCT-116 cells over-express autocrine PG (1–3,12), high concentrations of FAM-PG26 competed effectively with autocrine PG, perhaps reflecting higher binding-affinity of FAM-PG26 for CS-ANXA2 than PG (13), and/or rapid turnover of CS-ANXA2. Accumulation of FAM-PG26 was localized to focal areas of primary/metastatic tumors (Fig 2), which may reflect over-expression of CS-ANXA2 at these sites, as strongly suggested from results with ANXA2 staining of HEKmGAS xenografts (Supplementary-Figs 5C,D). Thus labeled/conjugated molecules with high-affinity for CS-ANXA2 may be useful for diagnosing/treating epithelial cancers.

Several signaling molecules/transcription factors are activated in target-cells in response to PG *in vitro* and *in vivo* (including:-

Src,PI3K,Akt,JAK2,STAT5/3,ERKs,p38MAPK,NFκB,β-catenin,Jagged1) (1,12,34–37). ANXA2 mediates signaling and proliferative effects of PG (7,11,12), and anti-ANXA2-Abs attenuate growth effects of exogenous/autocrine PG on pancreatic/colon-cancer cells (7,11). Current studies additionally demonstrate a significant (3–8fold) increase in relative-levels of potent transcription-factors (β-catenin/*p*NFκBp65) and stem/progenitor cell-markers (DCLK1/Lgr5/CD44) in HEKmGAS vs HEKC-cells, growing either as mono-layer cultures, 3D-spheroids or xenografts in mice (Figs 6A,B). Thus cells growing as 3D-structures *in vitro* and *in vivo* maintain parental expression profiles. Surprisingly, ratio of PG expression in HEKmGAS vs HEKC-cells significantly increased in spheroids/tumors compared to that in mono-layer cultures, suggesting the novel possibility that gastrin gene (PG) expression is up-regulated by factors (stress?) associated with 3D-growths. Percentage of stem/progenitor cells positive for DCLK1/CD44/Lgr5 were also significantly increased in HEKmGAS vs HEKC-cells in the order of CD44>DCLK1>Lgr5 (Fig 3). The most interesting finding was that almost all CS-ANXA2(+) cells co-expressed CD44 and vice versa (Figs 4D,E), suggesting that similar pathways may up-regulate cell-surface expression of CD44/CS-ANXA2.

The smallest CD44-isoform that lacks variant exons (CD44s) is abundantly expressed by normal and cancer cells, while variably glycosylated CD44v-isoforms (CD44v1-v10) are mainly expressed by cancer cells (38). Chondroitin-sulfate/heparin-sulfate modifications enables CD44v-isoforms to bind growth-factors/CS-ANXA2/MMPs (38–40), which dictates cellular-functions (migration/growth/survival) of CD44, as evidenced by loss of growth/metastasis of colonic-tumors, treated with anti-CD44v6-antibodies (41). Clustering of CD44 on tumor cells reportedly traps MMPs, which imparts invasive potential to epithelial cancer cells (40). At the same time, CS-ANXA2 expression is critically required for metastasis of tumors (14–16,18,42). CS-ANXA2 on hepatocellular-cancer-cells (HCC) (43), binds CD147-like-proteins resulting in secretion of MMPs and metastasis of HCC cells (18). Thus, CS-ANXA2 plays an equally important role in proliferation/metastasis of cancer-cells, which may be mediated by binding to specific ligands, such as tPA/plasminogen/PG/CD147 (11,12,14,15,18,42). Since both CS-ANXA2/CD44 appear to up-regulate/activate MMPs (as discussed above), significant increase in MMP2,7 levels in HEKmGAS vs HEKC-cells (Fig 5E), may reflect increased presence of CS-ANXA2/CD44 on cell-surface of HEKmGAS-cells (Fig 4). Surprisingly, down-regulation of ANXA2 attenuated MMP2,7 expression in HEKmGAS cells, by unknown mechanisms, which may have resulted in re-formation of rounded, less amorphous spheroids by HEKmGAS cells (Fig 5D); HEKC-cells, enriched for CS-ANXA2, on the other hand, developed amorphous-spheroids (Fig 5C). Based on our current understanding of interactions between CD44/CS-ANXA2/MMPs on tumor cells (as discussed above), it is speculated that loss or gain of CS-ANXA2/MMPs in CD44(+) stem-cells may impact metastatic behavior of cancer cells, and dictate morphology of spheroidal growths. In a recent study, down-regulation of Lgr5 in CRC-cells reportedly altered expression/distribution of MMPs/CD44, associated with invasion/migration of cells, resulting in formation of amorphous spheroids (44). The above findings support the novel concept that spheroid morphology may reflect tumorigenic/metastatic potential of cells. Additionally, in preliminary studies we have identified that the rim-like perimeter around wtHEKC-spheroids contains collagen IV (unpublished data from our laboratory), suggesting that non-transformed and perhaps some transformed stem cells retain the ability to lay down basement-like membranes around the spheroidal structures.

Several cell-surface markers have been used to identify colonic CSCs (including CD44,CD133,CD166,Lgr5,DCLK1) (22,45). Accumulating evidence suggests that CD133/CD166 may not be robust markers of cancer-stem-cells (CSCs) (45). CD44, however, is a strong marker for CSCs with a functional role in CSC biology (45), including cancer-cell

migration. Our results additionally suggest that CD44 and CS-ANXA2 may be co-expressed by highly tumorigenic/metastatic cells (Fig 4).

Functional role of Lgr5 in CSC biology remains unclear. Lgr5 expressing cells in small intestine generate structures resembling intestinal crypts *in vitro*, and intestinal tumors can arise from Lgr5(+) cells in APC mutant mouse models (21), suggesting Lgr5(+) cells may represent intestinal CSCs. Surprisingly, down-regulation of Lgr5 enhanced tumorigenesis of CRC cells, while over-expression of Lgr5 increased cell-cell adhesion (44). These confounding results provide evidence that Lgr5 may be a marker for CRC cells due to increased Wnt activity (supported by current findings); Walker et al (44) speculate that Lgr5 may regulate Wnt response and maintain colonic-crypt structures by inhibiting EMT. Since <20% CS-ANXA2(+) cells co-expressed Lgr5 (Fig 4), presence of CS-ANXA2 does not appear to be linked to expression of Lgr5, unlike co-expression of CD44/CS-ANXA2 (Figs 4D,E).

We observed that ~50% of CS-ANXA2(+)HEKmGAS cells co-expressed DCLK1 and >75% DCLK1(+)HEKmGAS cells co-expressed CS-ANXA2, suggesting a significant linkage between DCLK1/CS-ANXA2 expression (Figs 4D,E). DCLK1 is a microtubule-associated kinase and regulates spindle formation and mitotic cell-division in neuroblasts (46). Down-regulation of DCLK1 induces apoptosis in neuroblastoma cells (47). Thus DCLK1 plays an important role in neuroblastoma/neuronal biology. DCLK1 is up-regulated in CRC and down-regulation of DCLK1 results in growth arrest of tumors (22). Pancreatic cancer-stem-cells increasingly express DCLK1 and down-regulation of DCLK1 results in loss of c-Myc/Kras and EMT (23), suggesting that DCLK1 may play an important functional role in pancreatic/colorectal cancers. We similarly observed that down-regulation of DCLK1 significantly reduced proliferation of HEKC/HEKmGAS cells by ~50–70% (Fig 6D), suggesting that DCLK1 is required for maintaining growth of embryonic epithelial-cells as well. Our preliminary studies additionally suggest the novel possibility that DCLK1 is required for maintaining β-catenin activation (unpublished data from our laboratory).

DCLK1 expression levels were significantly increased in colonic-crypts of mice in response to elevated levels of circulating PG, resulting in hyperproliferation of colonic-crypts (12). In the current studies, we measured a significant increase in DCLK1(+) cells, co-expressing CS-ANXA2 and/or CD44 in HEKmGAS cells (Fig 4), which may represent a pool of highly tumorigenic/metastatic stem-cells.

Interestingly, DCLK1/Lgr5 staining cells were present mainly around perimeters of HEKC-spheroids, while CD44(+) cells were present both at the periphery and within the spheres, resembling Ki67 staining (Fig 5Bii). Co-expression of ANXA2with DCLK1was not observed in HEKC-spheroids (Supplementary-Fig 5A), resembling the profile seen in normal colonic crypts (12). Processing of HEKmGAS-spheroids resulted in loss of intact structures (Fig 5D), but the remaining clumps of HEKmGAS-spheroids co-stained for DCLK1/CD44 (Supplementary-Fig 5A), suggesting that the expression profile of transformed HEKmGAS stem-cells observed in 2D-cultures (Fig 4), is maintained in 3D-growths of HEKmGAS-cells.

In conclusion, we demonstrate a significant increase in % stem-cell populations co-expressing DCLK1/CD44/CS-ANXA2 in PG-overexpressing HEKmGAS-cells, in association with increased expression of MMPs which may contribute to increased tumorigenic/metastatic potential of HEKmGAS-cells and formation of amorphous-spheroids *in vitro*. Since almost all CD44(+)HEKmGAS cells, growing either as monolayer-cultures/ 3D- spheroids or xenografts, co-expressed CS-ANXA2 (Fig 4; Supplementary-Figs 5A,C,D), it is possible that co-expression of CD44/CS-ANXA2 by stem-cells may facilitate

growth/metastasis of transformed cells, and represent a hallmark (phenotype) of transformed stem cells. Previous and current findings confirm a functional role of DCLK1 for maintaining proliferation of normal/cancer cells; this may be linked to the surprising finding that β-catenin activation is attenuated in cells down-regulated for DCLK1 expression. Since down-regulation of either ANXA2, DCLK1 or CD44 (11,22,38, current studies) attenuates proliferative/tumorigenic/metastatic potential of transformed/cancer cells, targeting all three factors may provide an efficient approach for diagnosing/treating epithelial-cancers. Based on our findings we also postulate that labeled-ligands, demonstrating high-affinity for CS-ANXA2, may provide a selective tool for diagnosing/treating epithelial-cancers, since a majority of epithelial-cancers over-express CS-ANXA2 at leading edges of the tumors.

Supplementary Material

Refer to Web version on PubMed Central for supplementary material.

Acknowledgments

Grant Support: This work was supported by NIH grants CA97959 and CA114264 to PS and NASA grants NNX09AM08G and NNJ04HD83G to RU.

Abbreviations

Abs	antibodies
AnxA2	annexinA2
CD44	Cluster of differentiation44
co-IP	co-immunoprecipitation
CRC	colorectal cancer cells
CS-ANXA2	cell-surface associated annexinA2
CSCs	cancer stem cells
DCLK1	doublecortin-CAM-kinase-like1
EMT	epithelial-mesenchymal-transition
FACSorting	Fluorescence-activated cell sorting
FACScan	Fluorescence-activated cell scanning
FCS	fetal calf serum
HCT-116	human colorectal cancer cell line
HEKC	wtHEK-293 cells expressing control empty vector
HEKmGAS	HEK-293 clones overexpressing mutant gastrin gene resulting in expression of full-length progastrin
IF	Immunofluorescence
IHC	immunohistochemistry
Lgr5	Leucine-rich repeat-containing G-protein coupled receptor 5
Luc	firefly-luciferase
MMPs	matrixmetalloproteinases
NF-κB	nuclear factor-κB

p65	p65NF-κB
PG	progastrin
shRNA	small hairpin RNA
siRNA	small inhibitory double stranded RNA Oligonucleotides
Sup	Supplementary
vs	versus
WB	western blot

References

1. Rengifo-Cam W, Singh P. Role of progastrins/gastrins and their receptors in GI and pancreatic cancers: targets for treatment. Curr Pharm Des. 2004; 10:2345–58. [PubMed: 15279613]
2. Singh P, Owlia A, Varro A, Dai B, Rajaraman S, Wood T. Gastrin gene expression is required for proliferation and tumorigenicity of human colon-cancer-cells. Cancer Res. 1996; 56:4111–15. [PubMed: 8797575]
3. Smith JP, Verderame MF, Ballard EN, Zagon IS. Functional significance of gastrin gene expression in human cancer-cells. Regul Pept. 2004; 117:167–73. [PubMed: 14749036]
4. Wang TC, Koh TJ, Varro A, Cahill RJ, Dangler CA, Fox JG, Dockray GJ. Processing and proliferative effects of human progastrin in transgenic mice. J Clin Invest. 1996; 98:1918–29. [PubMed: 8878444]
5. Baldwin GS, Hollande F, Yang Z, Karelina Y, Paterson A, Strang R, Fourmy D, Neumann G, Shulkes A. Biologically active rhuman progastrin(6–80) contains a tightly bound calcium ion. J Biol Chem. 2001; 276:7791–96. [PubMed: 11113148]
6. Singh P, Lu X, Cobb S, Miller BT, Tarasova N, Varro A, Owlia A. Progastrin1–80 stimulates growth of intestinal epithelial cells in vitro via high-affinity binding sites. Am J Physiol. 2003; 284:G328–39.
7. Rengifo-Cam W, Umar S, Sarkar S, Singh P. Anti-apoptotic effects of progastrin on pancreatic cancer-cells are mediated by sustained activation of nuclear-factor-{kappa}B. Cancer Res. 2007; 67:7266–74. [PubMed: 17671195]
8. Singh P, Velasco M, Given R, Varro A, Wang TC. Progastrin expression predisposes mice to colon carcinomas in response to chemical carcinogen. Gastroenterology. 2000; 119:162–71. [PubMed: 10889165]
9. Cobb S, Wood T, Ceci J, Varro A, Velasco M, Singh P. Intestinal expression of mutant and wild-type progastrin increases colon-carcinogenesis in response to azoxymethane in transgenic mice. Cancer. 2004; 100:1311–23. [PubMed: 15022301]
10. Jin G, Ramanathan V, Quante M, Baik GH, Yang X, Wang SS, Tu S, Gordon SA, Pritchard DM, Varro A, Shulkes A, Wang TC. Inactivating cholecystokinin-2 receptor inhibits progastrin-dependent colonic-crypt fission, proliferation, and colorectal-cancer in mice. J Clin Invest. 2009; 119:2691–701. [PubMed: 19652364]
11. Singh P, Wu H, Clark C, Owlia A. AnnexinII binds progastrin and gastrin-like peptides, and mediates growth factor effects of autocrine and exogenous gastrins on colon-cancer and intestinal-epithelial-cells. Oncogene. 2007; 26:425–40. [PubMed: 16832341]
12. Sarkar S, Swiercz R, Kantara C, Hajjar KA, Singh P. AnnexinA2 mediates up-regulation of NF-κB, β-catenin, and stem-cells in response to progastrin in mice and HEK-293 cells. Gastroenterology. 2011; 140:583–95. [PubMed: 20826156]
13. Sarkar S, Singh P. Endosomal translocation of progastrin/AnnexinII is required for measuring activation of p38MAPK/ERK/NFκBp65 in IEC-18 cells. Gastroenterology. 2009; 138(Supplement-1):S-1987.

14. Díaz VM, Hurtado M, Thomson TM, Reventós J, Paciucci R. Specific interaction of tissue-type plasminogen activator with annexinII on membranes of pancreatic cancer-cells activates plasminogen and promotes invasion *in vitro*. Gut. 2004; 53:993–1000. [PubMed: 15194650]
15. Sharma M, Ownbey RT, Sharma MC. Breast cancer cell-surface annexinII induces cell migration and neoangiogenesis via tPA dependent plasmin generation. Exp Mol Pathol. 2010; 88:278–86. [PubMed: 20079732]
16. Zheng L, Foley K, Huang L, Leubner A, Mo G, Olino K, Edil BH, Mizuma M, Sharma R, Le DT, Anders RA, Illei PB, Van Eyk JE, Maitra A, Laheru D, Jaffee EM. Tyrosine 23 phosphorylation-dependent cell-surface localization of annexinA2 is required for invasion and metastases of pancreatic cancer. PLoS One. 2011; 6:e19390. [PubMed: 21572519]
17. Dontu G, Abdallah WM, Foley JM, Jackson KW, Clarke MF, Kawamura MJ, Wicha MS. In vitro propagation and transcriptional profiling of human mammary stem/progenitor cells. Genes Dev. 2003; 17:1253–70. [PubMed: 12756227]
18. Zhao P, Zhang W, Tang J, Ma XK, Dai JY, Li Y, Jiang JL, Zhang SH, Chen ZN. Annexin II promotes invasion and migration of human hepatocellular-carcinoma-cells in vitro via its interaction with HAb18G/CD147. Cancer Sci. 2010; 101:387–95. [PubMed: 20047591]
19. Ottewell PD, Varro A, Dockray GJ, Kirton CM, Watson AJ, Wang TC, Dimaline R, Pritchard DM. COOH-terminal 26 amino-acid residues of progastrin are sufficient for stimulation of mitosis in murine colonic epithelium in vivo. Am J Physiol. 2005; 288:G541–49.
20. Kesavan K, Ratliff J, Johnson EW, Dahlberg W, Asara JM, Misra P, Frangioni JV, Jacoby DB. AnnexinA2 is a molecular target for TM601, a peptide with tumor-targeting and anti-angiogenic effects. J Biol Chem. 2010; 285:4366–74. [PubMed: 20018898]
21. Barker N, Clevers H. Leucine-rich repeat-containing G-protein-coupled receptors as markers of adult stem cells. Gastroenterology. 2010; 138:1681–96. [PubMed: 20417836]
22. Sureban SM, May R, Ramalingam S, Subramaniam D, Natarajan G, Anant S, Houchen CW. Selective blockade of DCAMKL-1 results in tumor growth arrest by Let-7a MicroRNA-dependent mechanism. Gastroenterology. 2009; 13:649–59. [PubMed: 19445940]
23. Sureban SM, May R, Lightfoot SA, Hoskins AB, Lerner M, Brackett DJ, Postier RG, Ramanujam R, Mohammed A, Rao CV, Wyche. DCAMKL-1 regulates epithelial-mesenchymal-transition in human pancreatic cells through miR-200a-dependent mechanism. Cancer Res. 2011; 71:2328–38. [PubMed: 21285251]
24. Singh P, Sarkar S, Umar S, Rengifo-Cam W, Singh AP, Wood TG. Insulin-like growth factors are more effective than progastrin in reversing proapoptotic effects of curcumin: critical role of p38MAPK. Am J Physiol. 2010; 298:G551–62.
25. Singh P. Role of AnnexinII in GI cancers: interaction with gastrins/progastrins. Cancer Lett. 2007; 252:19–35. [PubMed: 17188424]
26. Ma AS, Bel DJ, Mittal AA, Harrison HH. Immunocytochemical detection of extracellular-annexinII in cultured human skin keratinocytes and isolation of annexinII isoforms enriched in extracellular pool. J Cell Sci. 1994; 107:1973–84. [PubMed: 7983162]
27. Esposito I, Penzel R, Chaib-Harrireche M, Barcena U, Bergmann F, Riedl S, Kayed H, Giese N, Kleeff J, Friess H, Schirmacher P. Tenascin-C and annexinII expression in the process of pancreatic carcinogenesis. J Pathol. 2006; 208:673–85. [PubMed: 16450333]
28. Sharma MC, Sharma M. Role of annexinII in angiogenesis and tumor progression: a potential therapeutic target. Curr Pharm Des. 2007; 13:3568–75. [PubMed: 18220793]
29. Valapala M, Vishwanatha JK. Lipid raft endocytosis and exosomal transport facilitate extracellular trafficking of AnnexinA2. J Biol Chem. 2011; 286:30911–25. [PubMed: 21737841]
30. Ji NY, Park MY, Kang YH, Lee CI, Kim DG, Yeom YI, Jang YJ, Myung PK, Kim JW, Lee HG, Kim JW, Lee K, Song EY. Evaluation of annexin II as a potential serum-marker for hepatocellular-carcinoma using a sandwich ELISA method. Int J Mol Med. 2009; 24:765–71. [PubMed: 19885616]
31. Sarkar S, Maxwell CA, Luthra G, Singal A, Qui S, Bauer V, Okorodudu A, Singh P. AnnexinA2 is increasingly expressed and released into serum of patients positive for colonic growths in relation to disease progression: Diagnostic implications. Gastroenterology. 2011; 140(Supplement-1):S-341.

32. Patchell BJ, Wojcik KR, Yang TL, White SR, Dorscheid DR. Glycosylation and annexinII cell-surface translocation mediates airway epithelial wound repair. Am J Physiol. 2007; 293:L354–63.
33. Brumlik MJ, Daniel BJ, Waehler R, Curiel DT, Giles FJ, Curiel TJ. Trends in immunoconjugate and ligand-receptor based targeting development for cancer therapy. Expert Opin Drug Deliv. 2008; 5:87–103. [PubMed: 18095930]
34. Ferrand A, Bertrand C, Portolan G, Cui G, Carlson J, Pradayrol L, Fourmy D, Dufresne M, Wang TC, Seva C. Signaling pathways associated with colonic mucosa hyperproliferation in mice overexpressing gastrin-precursors. Cancer Res. 2005; 65:2770–77. [PubMed: 15805277]
35. Umar S, Sarkar S, Cowey S, Singh P. Activation of NF-kappaB is required for mediating proliferative/anti-apoptotic effects of progastrin on proximal colonic-crypts of mice, in vivo. Oncogene. 2008; 27:5599–611. [PubMed: 18521082]
36. Umar S, Sarkar S, Wang Y, Singh P. Functional cross-talk between beta-catenin and NFkappaB signaling pathways in colonic-crypts of mice in response to progastrin. J Biol Chem. 2009; 284:22274–84. [PubMed: 19497850]
37. Pannequin J, Bonnans C, Delaunay N, Ryan J, Bourgaux JF, Joubert D, Hollande F. The Wnt target jagged-1 mediates activation of notch signaling by progastrin in human colorectal-cancer-cells. Cancer Res. 2009; 9:6065–73. [PubMed: 19622776]
38. Misra S, Heldin P, Hascall VC, Karamanos NK, Skandalis SS, Markwald RR, Ghatak S. Hyaluronan-CD44 interactions as potential targets for cancer therapy. FEBS J. 2011; 278:1429–43. [PubMed: 21362138]
39. McVoy LA, Kew RR. CD44 and annexinA2 mediate C5a chemotactic cofactor function of vitamin D binding protein. J Immunol. 2005; 175:4754–60. [PubMed: 16177123]
40. Yu Q, Stamenkovic I. Localization of matrix-metalloproteinase-9 to cell-surface provides mechanism for CD44-mediated tumor invasion. Genes Dev. 1999; 13:35–48. [PubMed: 9887098]
41. Reeder JA, Gotley DC, Walsh MD, Fawcett J, Antalis TM. Expression of antisense CD44-variant6 inhibits colorectal tumor metastasis and tumor growth in a wound environment. Cancer Res. 1998; 58:3719–26. [PubMed: 9721884]
42. Ling Q, Jacovina AT, Deora A, Febbraio M, Simantov R, Silverstein RL, Hempstead B, Mark WH, Hajjar KA. AnnexinII regulates fibrin homeostasis and neoangiogenesis in vivo. J Clin Invest. 2004; 113:38–48. [PubMed: 14702107]
43. Longerich T, Haller MT, Mogler C, Aulmann S, Lohmann V, Schirmacher P, Brand K. AnnexinA2 as a differential diagnostic marker of hepatocellular-tumors. Pathol Res Pract. 2011; 207:8–14. [PubMed: 20971570]
44. Walker F, Zhang HH, Odorizzi A, Burgess AW. LGR5 is a negative regulator of tumorigenicity, antagonizes Wnt signaling and regulates cell-adhesion in colorectal-cancer-cell lines. PLoS One. 2011; 6:e22733. [PubMed: 21829496]
45. Kemper K, Grandela C, Medema JP. Molecular identification and targeting of colorectal cancer-stem-cells. Oncotarget. 2010; 1:387–95. [PubMed: 21311095]
46. Shu T, Tseng HC, Sapir T, Stern P, Zhou Y, Sanada K, Fischer A, Coquelle FM, Reiner O, Tsai LH. Doublecortin-like-kinase controls neurogenesis by regulating mitotic spindles and M phase progression. Neuron. 2006; 49:25–39. [PubMed: 16387637]
47. Verissimo CS, Molenaar JJ, Meerman J, Puigvert JC, Lamers F, Koster J, Danen EH, van de Water B, Versteeg R, Fitzsimons CP, Vreugdenhil E. Silencing of microtubule-associated proteins doublecortin-like and doublecortin-like kinase-long induces apoptosis in neuroblastoma. Endocr Relat Cancer. 2010; 17:399–414. [PubMed: 20228126]

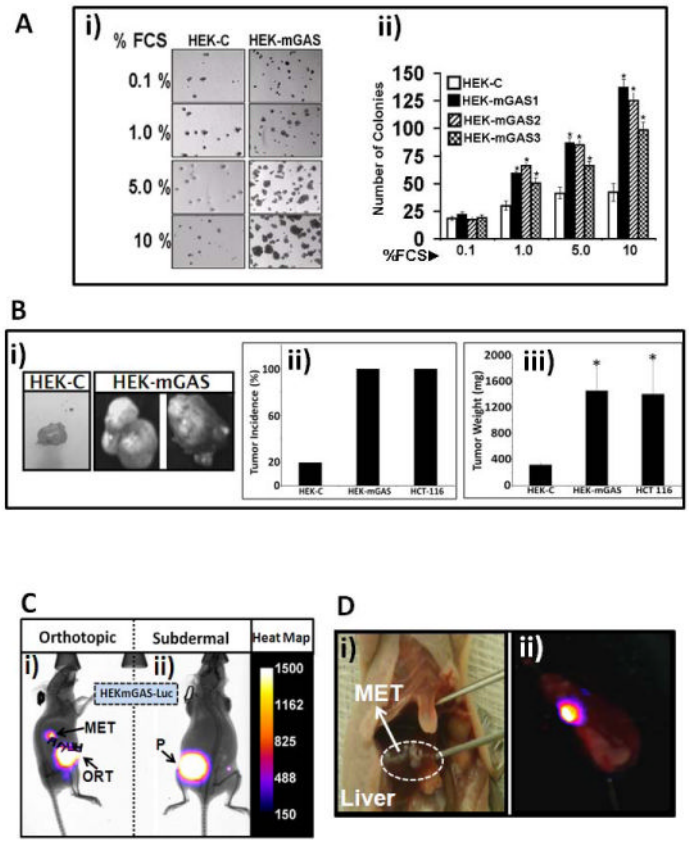

Figure 1. Clonogenic/tumorigenic/metastatic potential of HEKmGAS vs HEKC-cells

A. Clonogenic growth of HEKmGAS vs HEKC-cells on soft agar, in response to increasing concentration of FCS. **Ai**=Representative images of colonies/well; **Aii**=Mean±Sem of # of colonies/5 wells from indicated clones. **B.** Growth of HEKmGAS/HEKC-cells as sub-dermal tumors. **Bi**=Representative images of tumors formed from equal # of cells. **Bii**=% tumor incidence/10 inoculations/5 mice. **Biii**=Mean±Sem of tumor weights from either 2 (HEKC) or 10 (HEKmGAS/HCT-116) tumors, resected 6wks after inoculation. **C.** Representative bioluminescent images of mice bearing either orthotopic (ORT) cecal tumors with metastasis (MET), or sub-dermal (P, primary) tumors, derived from HEKmGAS-Luc cells; relative luminescence, gauged from the heat-map. **D.** Representative images of liver METs from mice inoculated intrasplenically with either HEKmGAS (**Di**=visual) or HEKmGAS-Luc (**Dii**=bioluminscent) cells.

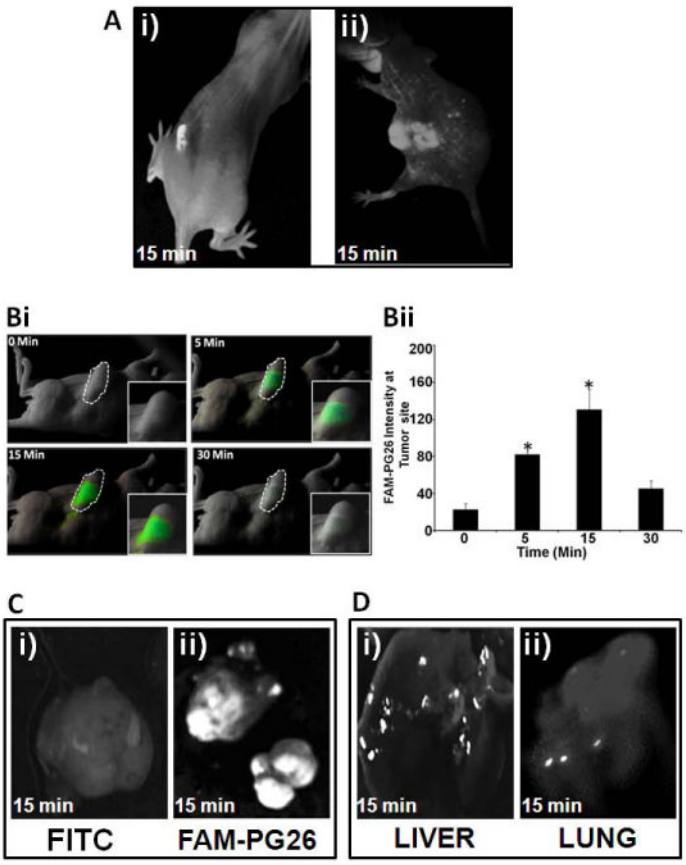

Figure 2. Detection of primary/metastatic tumors with FAM-PG26

Fluorescense detection of FAM-PG26 in tumors derived from HEKmGAS (**Ai,B,C,D**) and HCT-116 (**Aii**) cells. FAM-PG26 was injected either intratumorally (**Ai**) or in tail veins (**Aii,B,Cii,D**). Images were taken after indicated time-points either in intact anesthetized mice (**A,B**) or after resection of tumors/tissues(**C,D**). **(B)=**Time-dependent uptake of FAM-PG26 by sub-dermal tumors. **Bi**= fluorescent images from a representative mouse; **Bii**=Mean±Sem of relative fluorescence intensity at tumor site from 3 mice (described in Supplementary-Methods E). *=$p<0.05$ vs 0min values. **(Ci,Cii)=**sub-dermal tumors from mice injected with either FITC (**Ci,** control) or FAM-PG26 **(Cii). (D)**=liver/lung samples containing metastatic-lesions from mice injected with FAM-PG-26.

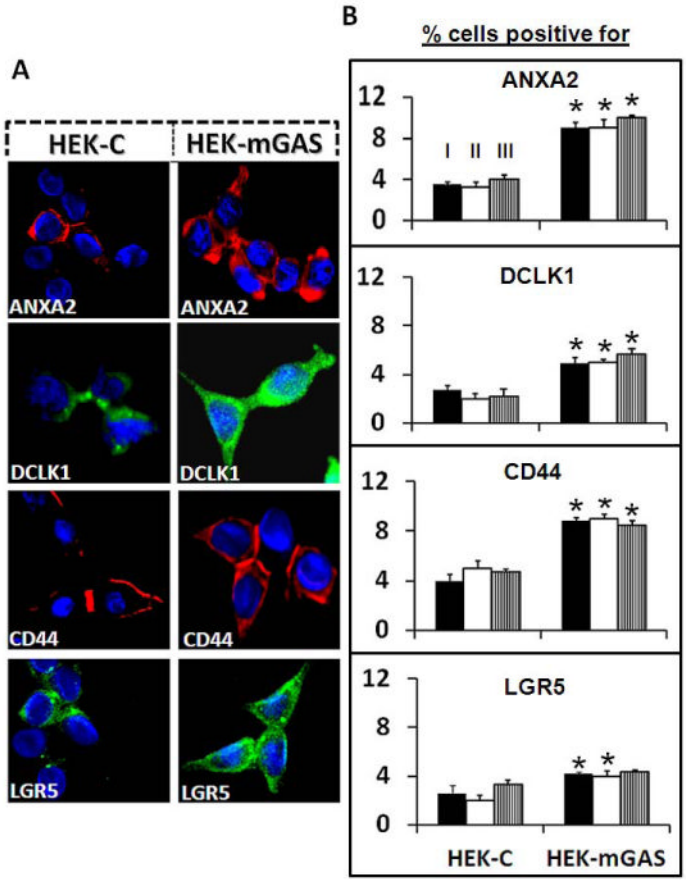

Figure 3. HEKmGAS vs HEKC-cells positive for ANXA2/DCLK1/CD44/Lgr5

A=Representative images of cells growing on glass slides, stained for the indicated proteins (40x). **B**=% cells positive for the indicated proteins were measured independently by the 3 separate methods (I-III, as labeled on the first set of bar-graphs in the top panel, as described in Supplementary-Fig 3A); bar-graphs=Mean±Sem of 3–4 experiments. *=$p<0.05$ vs HEKC values.

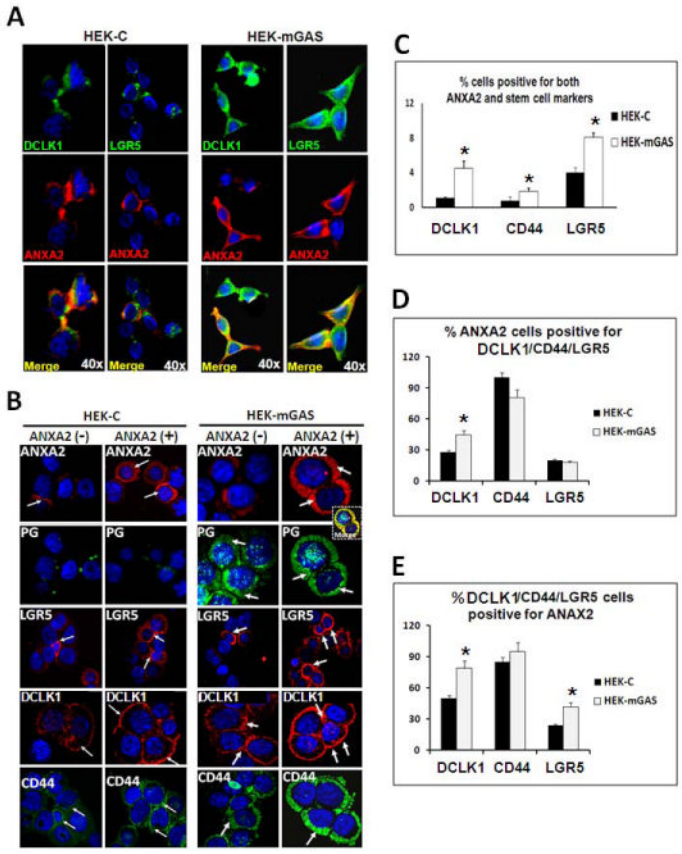

Figure 4. Expression of stem-cell-markers and ANXA2/CS-ANXA2 in HEKmGAS/HEKC-cells

A=Representative images of cells growing on cover-slips (Method II), stained for indicated proteins. **B**=Representative images of cells (from 2–3 experiments), FACSorted for ANXA2(−)/ANXA2(+) populations after staining for the indicated proteins; images from a wider field shown in Supplementary-Fig 4. Co-localization of ANXA2/PG in CS-ANXA2(+)HEKmGAS cells is shown in inset (yellow image). Arrows highlight staining. **C–E**=% cells co-expressing ANXA2 and the indicated stem-cell-markers were calculated as described in Supplementary-Method (G); results are presented as Mean+Sem from 2–3 experiments. *=$p<0.05$ vs HEKC values.

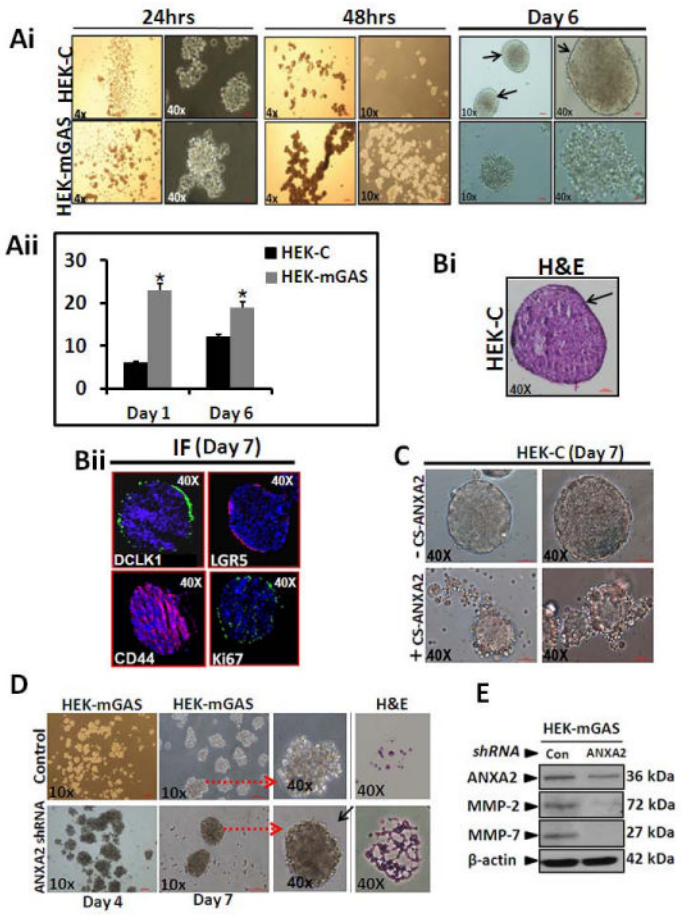

Figure 5. Morphology of HEKC/HEKmGAS spheroids in presence or absence of ANXA2 expression; effect on MMP levels

Ai=Cell growth in non-adherent cultures after indicated time-points. **Aii**=Each bar graph represents mean±SEM of total number of spheroids/well in 6 well plates for HEKmGAS vs HEKC-cells from two separate experiments, at indicated time-points. **Bi,Bii**=Representative images of H&E/IF stained sections (5μm) from HEKC-spheroids. **C**=HEKC-cells, FACSorted for presence(+) or absence(−) of CS-ANXA2, and grown as spheroids, using equal # of cells; representative images at day 7. **D**=Representative images of spheroids from HEKmGAS-cells, transfected with either control or ANXA2-shRNA plasmids; H&E stained spheroid sections shown in the last panel. Arrows point to enhanced images. **E**=relative levels of indicated proteins by WB analysis of HEKmGAS-spheroids in **D** (day 7); data is representative of 4 blots from 2 experiments.

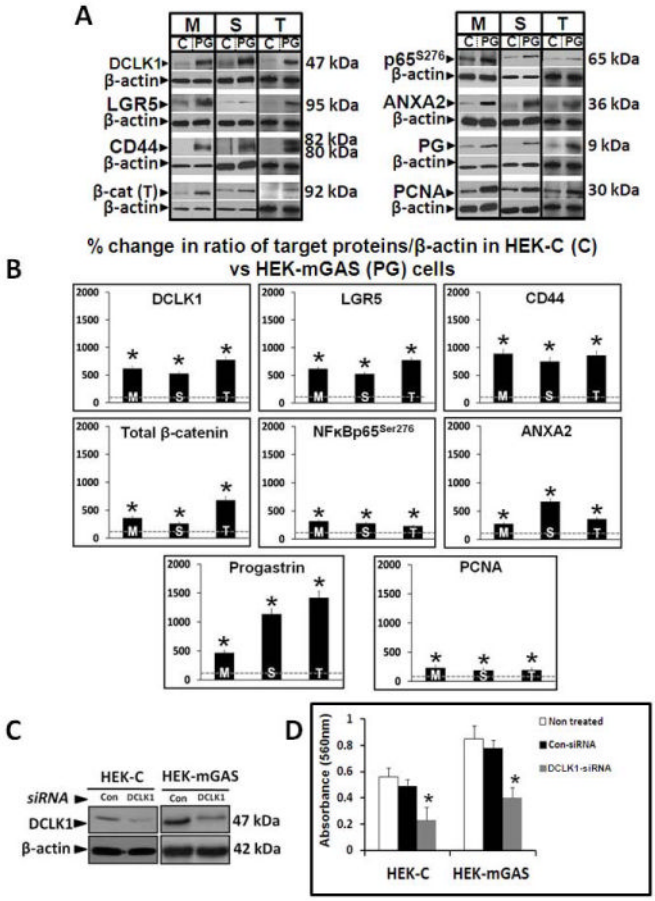

Figure 6. A,B. Percent increase in relative levels of stem-cell-markers, β-catenin/*p*NFκBp65, ANXA2/PG and PCNA in monolayer-cultures (M), 3D-spheroids (S) or sub-dermal tumors (T) of HEKmGAS vs HEKC-cells

A=Representative WBs of indicated proteins from 1 of 3 similar experiments; C=HEKC-cells; PG=HEKmGAS-cells. **B=**Mean±Sem of % change in ratio of indicated protein/β-actin in cellular samples from 3 experiments; ratios measured in HEKC samples were arbitrarily assigned 100% values. *=p<0.05 vs HEKC values (shown as dashed lines in each panel). β-cat (T)=total cellular levels of β-catenin. Figures 6D,C. Down-regulation of DCLK1 significantly reduces growth of HEKC/HEKmGAS cells. C=representative autoradiogram of WB data from 1 of 3 experiments, demonstrating relative levels of DCLK1 in cells treated with either control (Con) or DCLK1 specific siRNA; β-actin run as a loading control. **D**=growth (in terms of absorbance in an MTT assay) of indicated cells; each bar-graph=Mean±Sem of data from 8 wells/2experiments.